Contents lists available at ScienceDirect

Solar Energy Materials & Solar Cells

Effects of Ti-incorporation in CuInS$_2$ solar cells

Björn Marsen [a,*], Lars Steinkopf [a], Abhishek Singh [a], Helena Wilhelm [a], Iver Lauermann [b],
Thomas Unold [a], Roland Scheer [a], Hans-Werner Schock [a]

[a] Solar Energy Research/Technology, Helmholtz-Zentrum Berlin für Materialien und Energie, Hahn-Meitner-Platz 1, 14109 Berlin, Germany
[b] Solar Energy Research/Heterogeneous Materials Systems, Helmholtz-Zentrum Berlin für Materialien und Energie, Hahn-Meitner-Platz 1, 14109 Berlin, Germany

ARTICLE INFO

ABSTRACT

Titanium has been incorporated in CuInS$_2$ thin films and devices by diffusion of Ti from the substrate during the CuInS$_2$ co-evaporation growth process. The CuInS$_2$ crystal structure is unaffected but the grain size is reduced compared to Ti-free reference samples. X-ray photoelectron spectroscopy shows the presence of TiO$_2$ at the front of the absorber layer, which appears at the heterojunction interface of the completed CuInS$_2$/TiO$_2$/CdS/ZnO solar cells. Low temperature photoluminescence spectra show no additional transitions that could be assigned to Ti-based impurity defect levels. Ti-containing cells show conversion efficiencies higher than the Ti-free reference cells due to higher open-circuit voltage (efficiency 11%, $V_{OC}=731$ mV). No reduction in short circuit current is detected, indicating that the titanium does not introduce additional bulk recombination. Temperature-dependent current-voltage measurements indicate a reduced interface recombination for cells containing Ti, which is attributed to the TiO$_2$ interlayer detected by X-ray photoelectron spectroscopy.

1. Introduction

The incorporation of Ti in a chalcopyrite-structure semiconductor has been suggested for the formation of an intermediate band (IB) [1] and studied theoretically by electronic structure calculations [1–5] and solar cell calculations [6]. The calculated density-of-states of a CuGaS$_2$-derived structure, where 25% of the Ga atoms are substituted by Ti, shows the formation of an intermediate band near the center of the fundamental bandgap [1]. At high Ti concentration, the substitution is calculated to be thermodynamically less stable than the decomposition into Cu$_{0.6}$TiS$_2$ and CuGaS$_2$ [7]. However, it is possible that a metastable Ti-containing material can be synthesized in a kinetically controlled reaction. To the authors' knowledge, there have not been any experimental studies on the incorporation of Ti in chalcopyrite materials. Although a material with a wide bandgap such as CuGaS$_2$ (2.4 eV) would be the prefered host material for the implementation of intermediate band solar cells, for this study CuInS$_2$ is chosen as a model system since it can be prepared with much higher electronic quality at the moment. We focus on the incorporation of trace amounts of titanium in device quality CuInS$_2$ thin films and solar cells, in order to study the mode of incorporation and its effect on devices. In the present approach, solar cells are fabricated in the Mo/CuInS$_2$/CdS/ZnO device structure [8], which is distinct from TiO$_2$/CuInS$_2$ nanocomposite

solar cell in which the TiO$_2$ functions as the n-type part of the heterojunction [9]. Introducing a low concentration of Ti by diffusion from the back contact during co-evaporation CuInS$_2$ growth, the effects on the structure and properties of the absorber layer are investigated by scanning electron microscopy, X-ray diffraction, secondary ion mass spectrometry, X-ray photoelectron spectroscopy (XPS), and photoluminescence spectroscopy. The effects of the Ti-incorporation on solar cells are studied by illuminated current–voltage measurements at room temperature and at variable temperatures from 50 to 300 K.

2. Experimental

Glass substrates sputter-coated with a 0.5 μm Mo layer were used as substrates for all samples in this study. Substrates of the "Ti" group were additionally coated with a 10 nm Ti layer by electron-beam evaporation. The CuInS$_2$ absorber layers were grown on "Ti" and "Ref" substrates in a 2-stage co-evaporation process using elemental copper- and indium-sources and a sulfur source with cracking zone. An initial In–S deposition step at 275 °C substrate temperature was followed by Cu–S evaporation at 600 °C substrate temperature, resulting in 2–3μm thick CuInS$_2$ films with a surface segregation of CuS [8]. The CuS was removed by KCN etch. Solar cells were fabricated from such absorber samples by CdS chemical bath deposition, ZnO sputter deposition, and Ni/Al grid deposition.

Cross sections of absorber samples were imaged in a LEO 1530 scanning electron microscope (SEM) at 3 kV acceleration voltage

* Corresponding author. Tel.: +49 30 8062 2678; fax: +49 30 8062 2931.
E-mail address: bjoern.marsen@helmholtz-berlin.de (B. Marsen).

and 3–4 mm working distance, using the in-lens detector. Secondary ion mass spectrometry (SIMS) depth profiles of complete cells were recorded on a Cameca IMS 6f. With a primary beam of 8 keV O^{2-} ions, depth profiles were recorded for ^{65}Cu, ^{198}Mo, and ^{48}Ti secondary ions. The Ti trace was calibrated based on an $CuInS_2$:Ti standard implanted with a known Ti dose. Analysis by X-ray photoelectron spectroscopy (XPS) was performed on a TiO_2 film, a TiS_2 crystal, a reference $CuInS_2$ and a "Ti" group $CuInS_2$ sample. The latter sample had the cover layer of CuS removed in a glove box under inert gas atmosphere, followed by the direct transfer into the ultrahigh vacuum XPS chamber without exposure to air. Photoelectrons were excited by Al Kα radiation from an anode operated at 250 W.

Illuminated current–voltage curves of complete solar cells were recorded at room temperature under a "Solar Constant 575" solar simulator (K.H. Steuernagel Lichttechnik). The illumination intensity was set based on a GaAs reference cell calibrated at the Fraunhofer Institute Solar Energy Systems (ISE). Temperature- and illumination-dependent current–voltage curves were measured in a cryostat from 50 to 300 K, using a set of neutral density filters to obtain different attenuation levels of the solar simulator light.

3. Results and discussion

3.1. Structure and composition

Secondary electron micrographs of sample cross sections grown with (B) and without titanium (A) are shown in Fig. 1. The images indicate that the typical grain size in the Ti-free sample is on the micrometer scale whereas the grains of the Ti-containing sample appear smaller. The presence of Ti inhibits the formation of larger grains typical for $CuInS_2$ thin films grown under copper-rich conditions. X-ray diffraction measurements yielded identical patterns for both types of samples, as shown in Fig. 2. Apart from the ZnO and Mo signals from the auxiliary layers, they contain only roquesite ($CuInS_2$ chalcopyrite) peaks in almost identical proportions, suggesting that the dominant crystal structure of the films is unchanged by the incorporation of titanium.

The concentration depth profile of the Ti incorporated into the absorber layer was measured by dynamic SIMS. The depth profiles of Cu, Mo, and Ti are shown in Fig. 3. The Mo and Cu traces can be used to deduce reference points for the absorber front and back, as indicated by dashed lines in Fig. 3. The Ti trace was calibrated using an implanted $CuInS_2$:Ti sample. A Ti concentration of 10^{19}–10^{20} cm^{-3} is measured throughout the absorber. The higher signal at the back contact originates from the remainder of the Ti precursor. The enhanced Ti signal near the front of the absorber indicates diffusion of the Ti species in the growing $CuInS_2$ film. The average of the concentration inside the absorber of 8×10^{19} cm^{-3} corresponds to 0.04 at% or 400 ppm.

The chemical environment of the Ti atoms within 1 nm of the sample surface was probed by XPS. Photoelectron spectra around the Ti $2p_{3/2}$ peaks are shown in Fig. 4, for TiO_2, TiS_2, and Mo/$CuInS_2$ reference samples, and for a freshly prepared Mo/Ti/$CuInS_2$ sample. As the TiO_2 and TiS_2 spectra show, it can clearly be distinguished whether titanium is bound to sulfur or to oxygen. The spectrum of the TiS_2 sample also has weak shoulders reminiscent of the "Ti–O" peaks, which may be due to a surface oxidation of the sample. The spectra of both $CuInS_2$ samples show the In $3d_{3/2}$ peak at 452.5 eV binding energy. For the $CuInS_2$ film grown on Ti, the Ti $2p_{3/2}$ peaks are of equal intensity and in the same positions as for the TiO_2 sample. There is no indication of Ti–S bonds on that sample. This result suggests that a surface layer of TiO_2 is present on the $CuInS_2$ absorbers grown on Ti precursor.
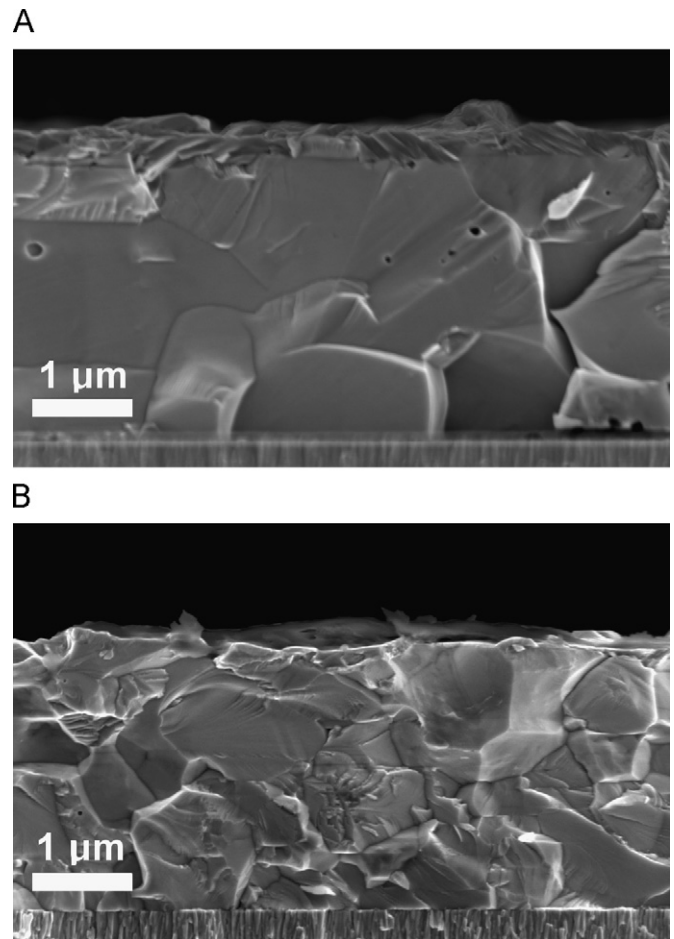

Fig. 1. Cross-sectional scanning electron micrographs of $CuInS_2$ films on (A) glass/Mo and (B) glass/Mo/Ti substrates.
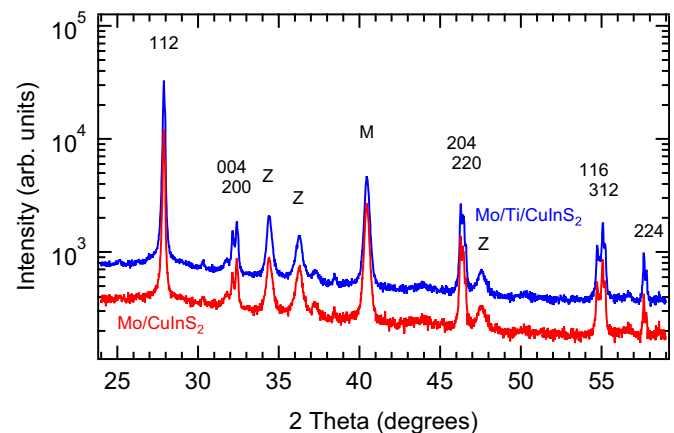

Fig. 2. X-ray diffraction data of $CuInS_2$ films on glass/Mo and glass/Mo/Ti substrates. Diffraction peaks that can be indexed to $CuInS_2$. Roquesite are labeled with their *hkl* indices, peaks arising from the molybdenum back contact and ZnO window layers are marked M and Z, respectively.

In order to detect new optically active defect centers in the $CuInS_2$ absorber possibly introduced by the Ti-incorporation, photoluminescence spectroscopy was applied to both "Ref" and "Ti" samples. The spectra are shown in Fig. 5. Both traces show prominently the donor–acceptor pair transition (In_i–VV_{Cu}) and its phonon replica at 1.39 and 1.35 eV, respectively. Also visible is the